CONTROL FEATURES OF A VECTORED-THRUSTER UNDERWATER VEHICLE

E. Cavallo, R. Michelini, V.F. Filaretov, D.A. Ukhimets

Italia, Genova, Telerobot srl,Italia, Genova, Università degli Studi di Genova, Russia, Institut for Automation and Control Process FEB RAS

Abstract: In the paper, control features of high-efficiency autonomous underwater vehicle (AUV) equipped by vectored thruster are considered. The original design of the three-degrees parallel mechanism is recalled. This mechanism allows to change the attitude of thrust's vector and, simultaneously, to compensate the screw-twist, applying a torque by means of an independent feedback loop. The control strategy of the thrust vector, applied through a 3DoF spherical mechanism is synthesised and investigated.

Keywords: underwater vehicle, high-quality three-dimensional control, position control, trajectory planning, control machinery

1. INTRODUCTION [1]

In the AUV designing, special attention is given to increase the manoeuvrability, to lower their overall size, and also to enhance the dynamic accuracy along any spatial trajectories (Amat J. at al. 1999).

As a rule, the modern AUV have several degrees of freedom, provided by iterating propellers of the same type (usually, from 4 up to 6). This considerably increases the vehicle weigh, external dimensions and hydrodynamic resistance. Therefore, the creation of new generation compact AUV is devised, exploiting the vectored-thruster concept, which makes the propeller to change spatial orientation by respect of the AUV longitudinal axis. This way, the resort to rudders is not required, avoiding the relevant growth of hydrodynamic resistance at fast AUV movement or the reduction of controllability at small speeds manoeuvring.

Earlier attempts of AUVs, with vectored thrusters, have already been investigated. E.g., in the work (Y.G. Le Page, K.W.Holappa 2000), a specially built two-degrees mechanism is considered; however, this lead to wobbly progression, as the exact orientation of the thrust vector in space is obtained, but not the simultaneous compensation of the drifting moment of the rotating propeller. On these premises, the present study (E.Cavallo, R.C.Michelini, V.F.Filaretov 2004) moves from the aim to implement a reliable and low-cost device, able to grant properly oriented thrust and to fully balance the screw torque. This required to simultaneously design: the 3 DoF mechanism, for the thruster actuation, and the control strategy providing the thrust vector with its exact spatial moving, with due concern of the task setting requirements.

2. TASK SETTING

The recalled aim lead to the Submarine Wobble-free Autonomous Navigator, SWAN, set-up, first of all, requiring to solve three separate subtasks:

- to create the device allowing to precisely oriented a thrust vector relative to its longitudinal axis and to compensate the disturbing moment due to propeller rotation;
- to develop the algorithm and control system of the three-degrees spherical parallel mechanism to change in space the (current) thruster's orientation;
- to check and investigate shrewd algorithms, control systems and trajectory planning laws of the vectored-thruster AUV, for the decision of various tasks in its mission space.

These three sub-tasks are basic issues, to assess the

This paper was supported by Russian foundation for basic research

SWAN feasibility and to acknowledge the operation benefits. A complex trajectory, notably in the marine environment with transverse and ascensional flows, requires inter-linked heaving and veering commands; wobbling is, further, controlled through a third loop, to keep the AUV moving, along the exact and steady space trajectory, as previously planned.

3. DEFINITION OF THE FORCE AND MOMENT APPLIED BY THE AUV VECTORED-THRUSTER

To select the vectored-thruster AUV control task, it is, at first, necessary to define forces and moments, applied to the AUV, by the propeller which generates the thrust T and the moment Q_T, opposite to screw rotation.

From fig. 1, it is visible, that the projections of vector T on the axes of the AUV coordinates system (CS) are given by the expressions:

$$T_x = T\cos(\delta_d)\cos(\delta_r), \quad T_z = T\cos(\delta_d)\sin(\delta_r),$$
$$T_y = T\sin(\delta_d), \qquad (1)$$

where δ_r, δ_d are deviation angles of the thruster axis from AUV longitudinal axis in the horizontal and vertical planes.

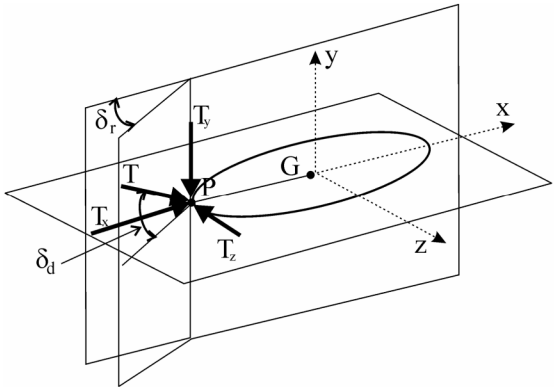

Fig. 1. Force and moment generated by the thrusters

The moments, created by the thrust vector T relative to the AUV centre of weight are calculated, in view of expressions (1), by the formulas:

$$M_y = T_z \times (\overline{PG}), \quad M_z = T_y \times (\overline{PG}), \qquad (2)$$

where $\overline{PG}$ is the vector directed from the application line of vector T to the AUV centre of mass.

The compensation of the moment Q_T can be given by two counter-rotating screws and two power supplies, on condition to control the co-ordination of the two propellers, when hydrodynamic disturbances apply. The SWAN setting splits power supply from control loops: the twist compensation is accomplished by an independent feedback, required to cancel the off-sets, rather than doubling the propulsion lines. This way, the AUV weigh and size are conveniently lowered, and the specially allotted control can easily adapt to any occurrence.

4. VECTORED-THRUSTER ACTUATION

To enable the SWAN idea, a special purpose wrist, derived by the spherical mechanism, described in the work (C.Gosselin, J.Angels, 1989), was designed and suitably adapted (E.Cavallo, R.C.Michelini, 2004). It consists of two frames, moving and fixed, connected, through revolute joints, by three identical two-links cinematic chains (see fig. 2). The axes of all joints cross in one point, the centre of the mechanism. The device has eight angular parameters: α_{1i} $(i = \overline{1,3})$, angles between vectors $\mathbf{u_i}$ and $\mathbf{w_i}$ of the i-th proximal link of the chain; α_{2i} $(i = \overline{1,3})$, angles between vectors $\mathbf{w_i}$ and $\mathbf{v_i}$ of the (i + 3), i-th distal link of the chain; β_1, angle that every vector $\mathbf{u_i}$ forms with the normal to the fixed frame; β_2, angle formed by vectors $\mathbf{v_i}$ and the normal to the moving frame.

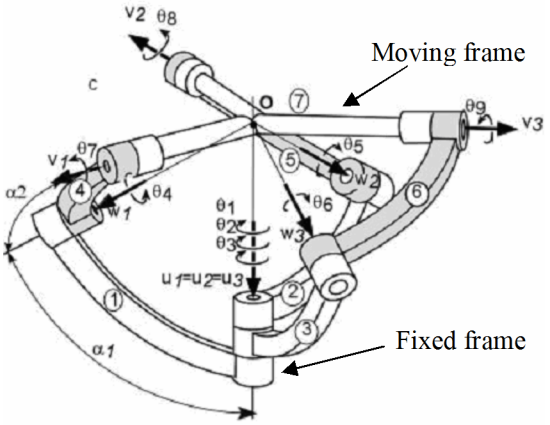

Fig. 2. Cinematic schema of the orientation device

The nine rotary joints describe the angles θ_i $(i = \overline{1,9})$. For the present application, the first three of them have the same rotation axis, coinciding with vectors $\mathbf{u_i}$ and are driven by the output shafts of three electric motors, all carried by the fixed frame. The vectors $\mathbf{w_i}$ $(i = \overline{1,3})$, in view of angles α_{1i} and α_{2i}, allow the full description of the rig. The vectors $\mathbf{v_i}$ $(i = \overline{1,3})$ are aligned with the rotating joints of the moving frame. Moreover, the vectors $\mathbf{u_i}$ are always parallel; $\beta 1=0$; and $\beta_2=\pi/2$; and, finally, the lay-out always keeps: $\alpha_{11}= \alpha_{12} = \alpha_{13}= \alpha_1$, and $\alpha_{21}= \alpha_{22}= \alpha_{23}= \alpha_2$.

The thruster actuation device is schematically shown in the fig. 3. placed on the AUV rear. The moving frame, driven by three planar rods, includes the inner bearing of the screw and the outer duct with external fins. The propeller is driven though a universal joint. The screw and the duct attitude, thereafter, modifies within a cone with angles α_1 and α_2 depending on the driving wrist. The duct, moreover, can continuously rotate, approximately powered by the three motors in parallel. Thus, the screw and the duct axes of rotation always coincide; the wrist allows large bends, limited at about $\pm$ 10°, in our case.

The finned duct rotation guarantees the screw torque compensation, making negligible the wobble, if the AUV is equipped with proper inertial sensors.

As far as the spherical wrist (see fig. 2) grants proper attitude to the thruster axis and suitable power to the finned duct, the SWAN idea enables a wobble-free motion, on condition to apply the appropriate control strategy through the three small electric motors, (see fig. 3).

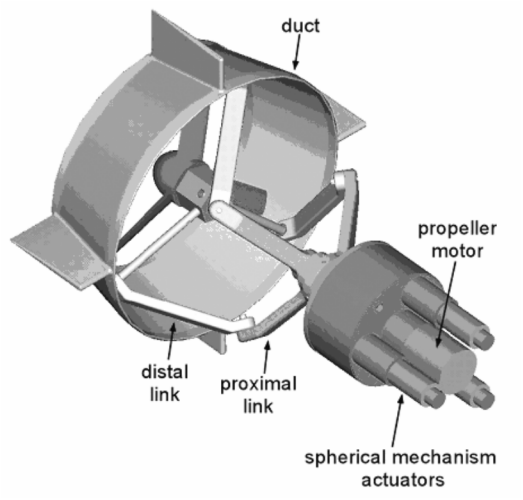

Fig.3. AUV thruster device

5. ORIENTATION DEVICE CONTROL SYSTEM

The backward kinematics is preliminary requirement for setting the AUV control; this links the vector T(t) orientation and rotation, α_j, with the corresponding angles $\theta_1(T)$, $\theta_2(T)$ and $\theta_3(T)$ of three electric motors. Moreover, the torque Q_d shall be supplied, to balance Q_T, with account of the screw thrust T(t), AUV speed **v**(t), hydrodynamic couplings and propeller type.

The multivariable model is translated into computer-oriented software (Maple7™, of WaterlooMaple Inc. and Matlab/Simulink™, of The Math Works Inc.), to assess the AUV dynamical behaviour for a sub-set of missions, through a simulation campaign (E.Cavallo, R.C.Michelini, V.F.Filaretov, D.A.Ukhimets 2004). This study brings to establish preliminary settings of the variables α_1 and α_2 law, leading to considerably lower the complexity of the analytical expressions to obtain each of the angles $\theta_i(T)$ $(i = \overline{1,3})$.

Basically, a PID-controller is used for the electrical motors actuation, to establish, both, the duct rotation and the vector T orientation. The combined input is:

$$\theta_i^*(t) = \theta_i(T,t) + \hat{\theta}_i(n,t) + \hat{\hat{\theta}}_i(\vartheta,t),$$

where: $\hat{\theta}_i(n,t)$, the current driving angles, in function of the screw rotation speed n, with due account of the duct rotation speed assuring the balancing moment Q_d with nominal mission setting; $\hat{\hat{\theta}}_i(\vartheta,t)$, the further angular correction, dependent on the current angle of roll ϑ, for veering manoeuvres (a similar correction applies for heaving manoeuvres, dependent on the pitch angle).
For the validation study (see fig. 2), the following example data are used: electric drives, with: R= 0.4 Ohm, L= $4\cdot10^{-3}$ Hn, active and inductive resistance of the DC motor anchor; K_ω= 0.02 Vs/rad, K_m= 0.02 Nm/A, counter electromotive force and motor torque coefficients; K_y = 400, amplifier gain; J= 10^{-4} kg·m^2, total moment inertia at the motor shaft; i= 100, gear ratio; M_T= 0.01 Nm, dry friction moment of the DC motor; b= 10^{-4} Nm·s/rad, viscous friction coefficient. The moment Q_T was assessed with the aid of (Fossen T.I., Blanke M., 2000); thus, the following thruster parameters and the surrounding viscous environment are obtained: D= 0.2 m screw diameter; ρ= 1025 kg/m^3, water density; K_Q= 0.015, non-dimensional torque coefficient.

The thruster axis position errors are shown in fig. 4; the axis orientation desired value follows a sine law. Curve 1 shows the tracking error with no feedback compensating the dry friction moments; curve 2, the error when this feedback is present. From the figure, it follows that the dry friction compensation, of the vector T orientation dynamic error, never exceeds 0.5 degrees, that, in many cases, is quite sufficient.

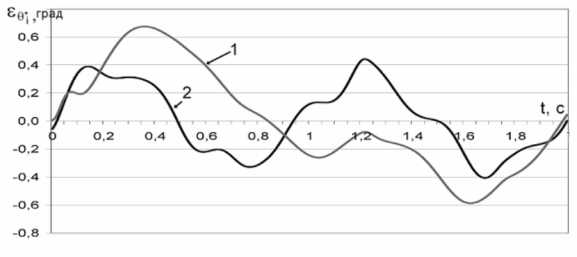

Fig.4. Error of position of thrust vector

The study confirms, since these preliminary issues, the effectiveness offered by the orienting mechanism, as the correcting devices grant exact enough tracking by positioning the AUV thruster axis. Therefore, the specified device can eventually be exploited, to build high-manoeuvrable and low-size AUVs, possessing minimal hydrodynamic resistance.

6. FEATURES OF THE **SWAN** CONTROL

To give further insight on the SWAN control, two missions of the AUV (shown in Fig. 5) are discussed:

- the approach to an object, with a pre-set orientation;
- the motion along complex spatial trajectories.

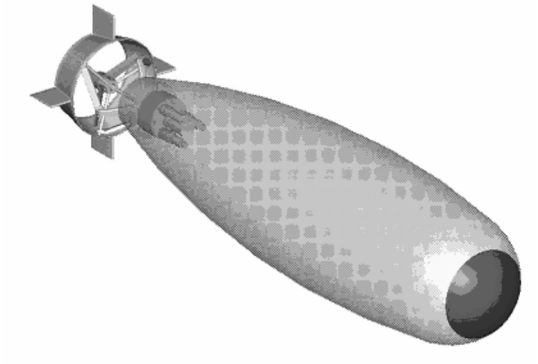

Fig. 5. Virtual model vectored-thruster AUV

6.1. Approaching an object with pre-set orientation

As the AUV has nonzero stability, good strategy is keeping a steady attitude in relation to some object O, along the approaching path with any speed. Let consider the mission in an horizontal plane, requiring the approach angle φ_0 (see fig. 6). To locate the AUV at the target point with the required docking angle to the object O, the path should comply two requests:

- the AUV needs travel, from some initial point A, to some point P_n , which lies in the horizontal plane of the object O, near to the object itself (see fig. 6);
- the AUV shall further turn in the horizontal plane, so to approach, with zero speed, the target P_0, with the desired orientation by respect to the object O.

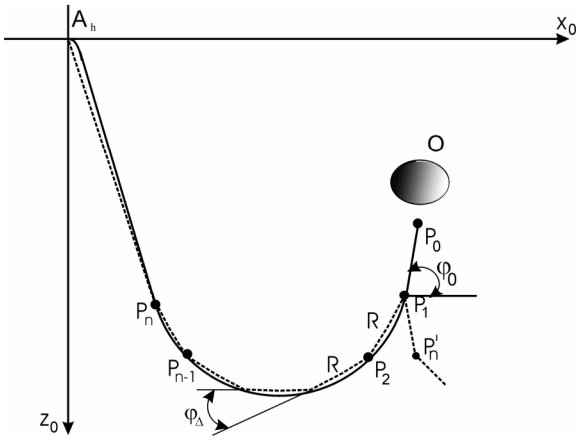

Fig. 6. Choice of the AUV approach path, with use of combined path and attitude control

Let's note, that, during the AUV motion, the current path slope is defined by the rate φ and trim ψ angles (if the goal is in a forward hemisphere), namely:

$$\varphi^* = -\text{arctg}\left((z_d - z)/(x_d - x)\right),$$
$$\psi^* = \text{arctg}\left((y_d - y)/(x_d - x)\right),$$

where: x_d, y_d, z_d, x, y, z are, respectively, the desired and the current AUV coordinates.

The AUV turning in the horizontal plane can be done by different laws. It is possible, for instance, to use the final position control, having chosen the series of turns at several intermediate points P_i $(i = \overline{n, 0})$ (see fig. 6), pre-setting the contour control on some circle arc P_nP_1 (see fig. 7). Thus, during the AUV motion to the object O, a combined path and attitude law will link back to individual initial point P_n, the AUV position and speed, assuring the required orientation.

The fig. 6 and 7 specify the AUV path projection in the X_0Z_0 horizontal plane, with the chosen bending law. The point A_h is the projection on the X_0Z_0 plane, of the AUV initial position A; the curve A_hP_n gives the projection on the same plane of the AUV motion. At first, we shall consider the AUV final position P_1, while docking at the object O, in the X_0Z_0 plane, from the point P_n (see fig. 6). Then, the intermediate points of the path P_i $(i = \overline{n-1, 1})$ are reckoned, giving the vertices of the broken line, at which the angle φ_Δ between adjacent strokes, changes, and the lengths R_L to be travelled with steady motion.

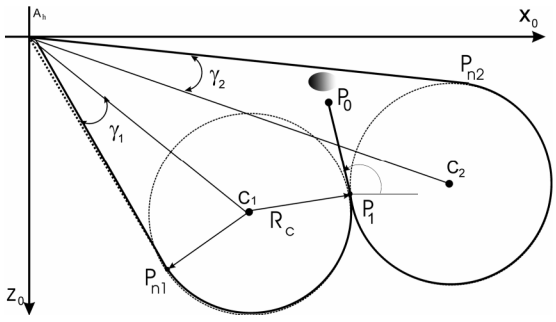

Fig. 7. Selecting the AUV approach path, by contour control

Then, the track P_1P_0 is the braking distance, covered by the AUV, to the object O, with the right docking angle φ_0. It is obvious, that the series of φ_Δ and R_L values depends on the AUV manoeuvrability and its local speed along the path. These data shall be pre-computed and checked during simulation. During the mission, the AUV consistently moves from point P_i of the broken line to point P_{i-1}, and turns to smoothly up-date the attitude; on last track P_1P_0, it receives the desired orientation to object O and stops at point P_0.

The coordinates of the AUV path intermediate points P_i of the and the corresponding desired turns φ_i at given points P_i of the broken line can be calculated from the final point P_0 (with coordinates $x_0 = x_d$, $y_0 = y_d$, $z_0 = z_d$) by means of the following expressions:

$$x_i = x_{i-1} - R_L\cos\varphi_i,\ z_i = z_{i-1} + R_L\sin\varphi_i,$$
$$\varphi_1 = \varphi_0,\ \varphi_{i+1} = \varphi_i + \varphi_\Delta,\ i = \overline{1, n},$$

where: $\varphi_\Delta = \varphi_{i-1} - \varphi_i$.

It is obvious, that, when computing the AUV motion in a horizontal plane (depending on the direction of turn to object), the value φ_Δ can accept both positive and negative values. Calculations of x_i, z_i and φ_i come to end at such values n at which the conditions are satisfied:

$$|\varphi_A - \varphi_n| \le |\varphi_\Delta|, \quad \text{if} \quad \varphi_A\varphi_n > 0,$$
$$||\varphi_A - \varphi_n| - 2\pi| \le |\varphi_\Delta|, \quad \text{if} \quad \varphi_A\varphi_n < 0.$$

Should the goal O be in the second or third quadrant, the current path slopes would be:

$$\varphi_A = -\text{arctg}\left((z_n - z_A)/(x_n - x_A)\right) - \pi,$$
$$\varphi_A = -\text{arctg}\left((z_n - z_A)/(x_n - x_A)\right) + \pi,$$

where: x_A, z_A, coordinates of the AUV initial position in the X_0Z_0 plane.

As before, the AUV turn trajectory in the horizontal plane is built, using a circle contour control. The path will follow a broken line, up to the location where

the correct docking angle is reached, and proper distance is left for braking. The radius of the circle and the AUV velocity come out from the dynamic properties of the set-up. It is obvious, that depending on the AUV turning direction, two circles are found (see fig. 7). The location of each subsequent circle arch $P_{n1}P_1$ is given by the expressions:

$$x_{P1} = x_{P0} - R_b\cos(\varphi_0),\ z_{P1} = z_{P0} + R_b\sin(\varphi_0),$$
$$x_{Pn1} = \sqrt{(x_{c1}-x_A)^2 + (z_{c1}-z_A)^2 - R_c^2}\times$$
$$\times\cos\left(\mathrm{arctg}\left((z_{c1}-z_A)/(x_{c1}-x_A)\right)\pm\gamma_1\right),$$
$$z_{Pn1} = \sqrt{(x_{c1}-x_A)^2 + (z_{c1}-z_A)^2 - R_c^2}\times$$
$$\times\sin\left(\mathrm{arctg}\left((z_{c1}-z_A)/(x_{c1}-x_A)\right)\pm\gamma_1\right),$$

where: $x_{c1} = x_{P1} - R_c\sin(\varphi_0),\ z_{c1} = z_{P1} - R_c\cos(\varphi_0)$,

$\gamma_1 = \arcsin(R_c/\sqrt{(x_{c1}-x_A)^2 + (z_{c1}-z_A)^2})$,

x_{p1}, z_{p1}, x_{pn1}, z_{pn1}, respectively, coordinates of points P_1 and P_{n1}.

The two possible ways, to set the same AUV docking at the object O with the desired attitude, present a similar difficulty. The example mission: *to approach, from the point* (0, 0, 0) *and* $\varphi = \psi = 0$, *the object* O, *located in the point* (50, 20,-50), is investigated. Three AUV motion modes were considered (see fig.8):

1. shortest path, with no constraint on the docking (curve 1 on the fig. 8);
2. docking to the object O, with angle $\varphi = \pi/2$ (curve 1 on the fig. 8);
3. docking to the object O, with angle $\varphi = -\pi/2$ (curve 1 on the fig. 8).

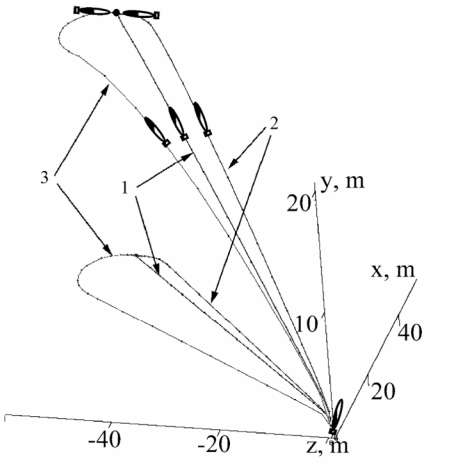

Fig. 8. Trajectories of AUV movement for the tree AUV motion modes

Two equal control blocks are used, to track ψ^* and φ^* angles along the AUV motion to the object; the block diagram of the one operating on the angle ψ, is shown in fig. 9. In this figure, the following notations are used: ε_ψ, tracking error on angle ψ; CD, typical correcting device; A, saturating amplifier; TCS, control block of three actuators; M_i, screw orienting motors (i= 1, 2, 3). CD is a PID-controller with transfer function: $W(s) = (T_1s^2 + T_2s + 1)/s$. The linear zone of the amplifier A has gain K_y.

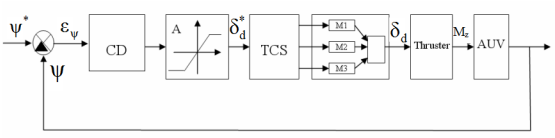

Fig. 9. Block diagram of the AUV trim angle control

In the study, the following example data are used for the AUV: m_a = 80 kg - total mass; J_{xx} = 2 kg·m^2, J_{yy} = = 10 kg·m^2, J_{zz} = 10 kg·m^2 – general inertia moments of AUV; d_{2x} = 25 kg·m^{-1}, d_{2y} = 125 kg·m^{-1}, d_{2z} = = 125 kg·m^{-1} – hydrodynamic coefficients of viscous friction; Y_c = 0.02 m – metacentric height; R_L = = 2.5 m; $\varphi_\Delta = 20^0$; $\delta_{dmax} = 25°$, $\delta_{rmax} = 25°$ - maximal values of deviation angles of orientation device; T_{max} = 100 N – maximal value of thrust, which generated by thruster. For the PID-controller: T_1 = = 0.02 s^{-1}, T_2 = 0.06 s^{-1}, K_y = 10.

On fig. 10, the φ and ψ angles trends are given, for the tree motion modes: for mode 1, curves 1, 2; for mode 2, curves 3 and 4; for mode 3, curves 5 and 6. The results clearly show that the AUV vectored-thruster can move to the desired point of the space with the required orientation.

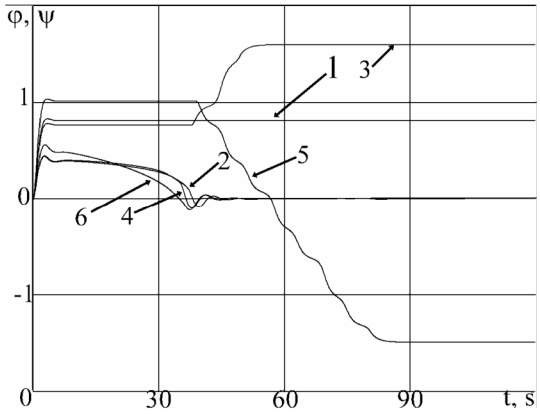

Fig. 10. Trends of φ and ψ angles for the tree AUV motion modes

6.2. AUV motion mode along random spatial paths

The exact AUV moving along a 3D path (see fig. 5) should take into account that heaving is possible only when moment M_z, created by thruster in the vertical plane overcomes the moment of stability:

$$M_{ost} = m_a g Y_c \sin(\psi), \qquad (3)$$

present if $\psi \neq 0$, where: g, gravity acceleration; Y_c, meta-centre height.

To overcome the moment M_{ost}, the needs have a forward velocity, exceeding a minimal value, defined by the angle ψ. Indeed, the thrust $T \neq 0$ and linked moment M_z, according to the expression (2), appear when the AUV moves with some velocity in the X axis direction. Then, to correctly establish the AUV

motion law, it is preliminary necessary to estimate the minimal forward velocity needed to track the requested angle $\psi \neq 0$.

Taking into account the expression (3), and recalling the square-law character of the hydrodynamic force in function of the AUV speed, this minimal velocity v_{xmin} is assessed as it follows:

$$v_{xmin} > \sqrt{m_a g Y_c \sin\psi / (|\overline{PG}| d_{2x} tg(\delta_{dmax}))} ,$$

where: δ_{dmax}, maximal thrust vector deviation angle in the vertical plane; d_{2x}, hydrodynamic coefficient in the x joint axes coordinate system; m_a, AUV mass.

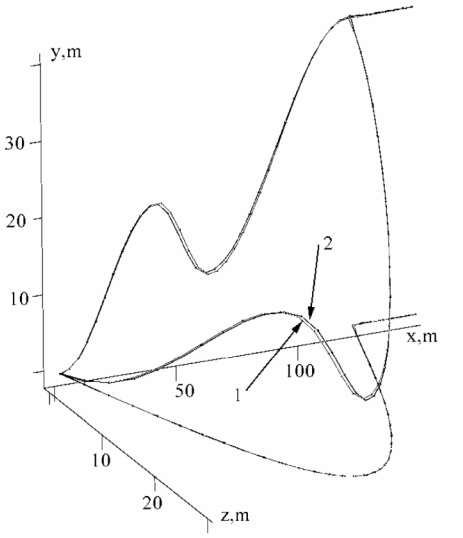

Fig. 11. AUV motion along 3D trajectories

Example simulation results the SWAN motion along spatial trajectories, are shown in fig. 11. In the figure, labels 1 and 2 show the planned and, respectively, the actual AUV paths, and their projections into the horizontal and vertical planes. The projection of AUV speed on the specified X_0 axis path was made equal to 1 m/s, leaving the absolute velocity variable. The results show that, for the specified AUV, the maximal deviation, of the actual from the planned motion, does never exceed 0.8 m.

CONCLUSIONS

In paper, the new concept of vectored-thruster AUV spatial movement control is prospected. The change of the thruster orientation, by respect to the AUV longitudinal axis, is carried out by the direct control of a spherical parallel mechanism. The same device provides the independent compensation of the screw torque on the AUV, using a counter-rotating finned duct. This bring to SWAN concept, leading to fix into a single control module the steering plans, fully avoiding drifting and wobbling disturbances.

Several control strategies of the specified AUV are developed, for veering and for heaving manoeuvres, along balanced and accurate 3D motion. The carried out mathematical models and computer simulations have fully confirmed the efficiency of the prospected approaches and the high dynamical accuracy of the SWAN-modified vectored-thruster AUV, even when very simple motion control laws are followed.

The SWAN idea, moreover, is expected to be very effective also when external disturbances apply, as the angular steering and torque balancing are directly accessed by independent loops, since three motors close the control. This leads to new studies, requiring a properly instrumented AUV.

REFERENCES

J. Amat, A. Monferrer, J. Batlle et al. (1999): “GARBI: a low-cost underwater vehicle”, *Microprocessors and Microsystems*. 1999. V. 23.

E. Cavallo, R.C. Michelini: “A robotic equipment for the guidance of a vectored thrustor AUV”, 35th Intl. Symposium on Robotics, ISR 2004, Paris, March 23-26, 2004, p. 88 (5) we 43-1.

E. Cavallo, R.C. Michelini, V.F. Filaretov: “Conceptual design of an AUV equipped with a 3dof vectored thrustor”, Intl. J. Intelligent and Robotic Systems, vol. 39, n. 4, April 2004, pp. 365-391, ISSN 0921 0296.

E.Cavallo, R.C.Michelini, V.F. Filaretov, D.A. Ukhimets: “Path guidance and attitude control of a vectored thrustor AUV”, 7th ASME Conf. Engineering Systems and Design Analysis, ESDA 2004, Manchester, 19-22 July 2004, ISSN 0143-991X.

T.I Fossen., M. Blanke (2000): “Nonlinear output feedback control of underwater vehicle propellers using feedback form estimated axial flow velocity”, *IEEE Journal of Oceanic Engineering*. V. 25. № 2.

C. Gosselin, J. Angeles (1989): “The optimum cinematic design of a spherical three-degrees of freedom parallel manipulator”, *ASME Mechanisms, Transmissions and Automation in Design*. V. 111.

Y.G. Le Page, K.W. Holappa (2000): “Simulation and control of an autonomous underwater vehicle equipped with a vectored thruster”, *The AUV 2000 Conference*, Pennsylvania State College, USA.